Multitwinned Spinel Nanowires by Assembly of Nanobricks *via* Oriented Attachment: A Case Study of Zn_2TiO_4

Yang Yang,*,† Roland Scholz,† Hong Jin Fan,‡ Dietrich Hesse,† Ulrich Gösele,† and Margit Zacharias§

†Max Planck Institute of Microstructure Physics, Weinberg 2, 06120 Halle, Germany, ‡Division of Physics and Applied Physics, School of Physical and Mathematical Sciences, Nanyang Technological University, 21 Nanyang Link, 637371 Singapore, and §IMTEK, Faculty of Applied Science, Albert-Ludwigs-University Freiburg, Georges - Köhler-Allee, 79110 Freiburg, Germany

ABSTRACT Nanowires with twinned morphology have been observed in many cubic-phase materials including spinel. We study systematically the formation of multitwinned Zn_2TiO_4 nanowires based on a solid−solid reaction of ZnO nanowires with a conformal shell of TiO_2, which is deposited by atomic layer deposition (ALD). By varying the solid-state reaction temperature, reaction time, and TiO_2 shell thickness, the formation process is carefully analyzed with the help of transmission electron microscopy. It is found that the multitwins develop through an oriented attachment of initially separated spinel nanobricks and a simultaneous Ostwald ripening process. The oriented assembly of the individual bricks is strongly dependent on annealing conditions, which is required to favor the motion and interaction of the bricks. This mechanism differs dramatically from those proposed for twinned nanowires grown with the presence of metal catalysts. Our result provides new insights on controlling the morphology and crystallinity of designed 1-D nanostructures based on a solid-state reaction route.

KEYWORDS: Zn_2TiO_4 · twin boundary · core−shell nanowires · solid−solid reaction · self-assembly · oriented attachment · Ostwald ripening

A twin boundary (TB) is a two-dimensional crystal defect and constitutes a special high-symmetry grain boundary.[1] A twinned interface consists of a single atomic plane, at which only the crystallographic orientations of two adjacent crystal domains change. As a result, usually no dangling bonds exist at their interface. From the viewpoint of TB genesis, twins are generally classified as growth twins, transformation twins, and mechanical or gliding twins. Given that the formation of TBs requires very little energy in many crystal structures like zinc blende and spinel, TBs occur commonly in various minerals.[1]

The structure and origin of TBs have been thoroughly investigated for more than two centuries.[1] Accompanying the rise of nanotechnology, increasing attention has been paid to the formation and structure of TBs in various nanostructures.[2−11] One-dimensional (1-D) semiconductor nanowires with very high surface area-to-volume ratio are very promising materials for electronic, photonic, mechanical, and chemical applications because of their unique electronic, optical, mechanical, and catalytic properties.[12−14] It was reported that the presence of a large number of crystal imperfections such as multi-TBs can limit the performance of optoelectronic nanowire devices.[6,15,16] In addition, it was found that in some occasions TBs could act as dislocation obstacles to affect the deformation behavior of nanostructures.[10,15,17] Designed elimination or creation of TBs during crystallization processes will give additional routes to fabricate new functional materials targeted to specific applications. Therefore, investigations on multitwins formed during crystal growth of 1-D semiconductor nanowires have attracted particular interests in recent years.[3−9]

In 2006 Johansson *et al.*[6] examined GaP nanowires with pseudoperiodical multitwinning structures grown by metal−organic vapor-phase epitaxy, and proposed that twin-plane nucleation is favored by fluctuations in mass transport as well as thermal fluctuations during vapor−liquid−solid (VLS) growth. Later, Zhang *et al.*[9] revealed that the lattice mismatch between the catalyst particle and the grown nanowire may be another contributing factor to the formation of multitwinning nanowires in some cases. Davidson *et al.*[7] systemically investigated multiple lamellar twins in GaAs, GaP, and InAs nanowires synthesized by supercritical fluid−liquid−solid (SFLS) and solution−liquid−solid (SLS) approaches. In their studies, a semiquantitative model was developed, elucidating that twinning depends on the ability of the contact angle at the three-phase boundary to fluctuate enough to accommodate the sidewall

*Address correspondence to yangyang@mpi-halle.de.

Received for review October 13, 2008 and accepted February 23, 2009.

Published online March 3, 2009.
10.1021/nn800681q CCC: $40.75

faceting of a twinned plane nucleated at the nanowire tip.[7] The above contributions basically reveal the formation mechanism of multitwinning semiconductor nanowires grown by VLS, SFLS, and SLS processes, in which a seed metal catalyst is involved to promote semiconductor nanowire growth. There are only a few reports on fabrications of multitwinned nanowires *via* a catalyst-free approach. Recently, Yang *et al.*[8] reported the synthesis of multitwinned Zn_2TiO_4 ternary oxide nanowires by reacting ZnO nanowires with a magnetron-sputter-deposited stoichiometric metal Ti layer. Structurally the sputter-deposited Ti layer was not conformal. Furthermore, the electron and ion bombardment during the sputter process caused concentration fluctuations in the ZnO nanowires prior to the high temperature solid−solid reaction. It was concluded that these two types of unavoidable nonuniformity probably contributed to the formation of multitwinned Zn_2TiO_4 nanowires. However, the formation mechanism suggested by Yang *et al.* was only hypothetic and the science behind it has still not yet been resolved.

In the current work, we will investigate the formation of Zn_2TiO_4 multitwinned nanowires using single-crystalline ZnO nanowires as a reactive template. Unlike the work by Yang *et al.*,[8] we coat a very thin and uniform TiO_2 film around ZnO nanowire cores by atomic layer deposition (ALD). It is known that ALD is a relatively mild deposition method that allows conformal coating and precise thickness control without destroying the surface.[18] On the basis of the controlled solid-state reaction of these 1-D ZnO/TiO_2 core−shell nanowires with a uniform interface, we are able to reveal the general mechanism of multitwinned nanowires formed *via* a solid−solid reaction of 1-D core−shell nanostructures. Our result is not only useful to the understanding of twin boundary formation in nanostructures, but also provides new information on how to control the crystallinity of nanowires *via* designed solid-state reactions.

RESULTS AND DISCUSSION

General Morphology of the Multitwinned Nanowires. The as-grown ZnO nanowires prepared by gold-catalyzed vapor-phase transport in this experiment grew along the [0001] direction.[19] The diameter of the ZnO nanowires is in the range of 60−200 nm. An overview of the ZnO nanowires after depositing titania by applying 300 ALD cycles is shown in a TEM image (Figure 1a), where individual nanowires with different diameters can clearly be observed. From a high magnification TEM image shown in Figure 1b, a smooth TiO_2 film with a uniform thickness of ~5 nm is found to coat the surface of ZnO, forming ZnO/TiO_2 core−shell coaxial nanowires. The as-deposited TiO_2 film is primarily amorphous because of the relatively low deposition temperature (100 °C). However, this amorphous phase can

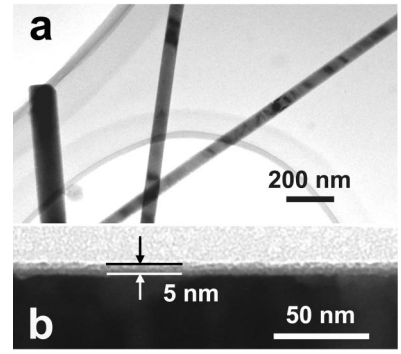

Figure 1. (a, b) TEM images of core−shell ZnO/TiO_2 nanowires obtained by atomic layer deposition of ~5 nm TiO_2 film around ZnO nanowires.

transform into crystalline TiO_2 films by a subsequent annealing step at temperatures of more than 300 °C.[20]

A high-temperature solid-state reaction or high-energy ball milling of a ZnO/TiO_2 mixture has been reported for the fabrication of zinc titanate nanocrystallites.[21,22] To induce the interfacial solid−solid reaction for the formation of Zn_2TiO_4 spinel based on our ZnO/TiO_2 core−shell nanowires, we annealed the samples at 900 °C for 8 h in an open furnace. After the reaction, a large fraction of nanowires transformed into zigzag structures, as presented in Figure 2a. Moreover, the diameter of the annealed nanowires is re-

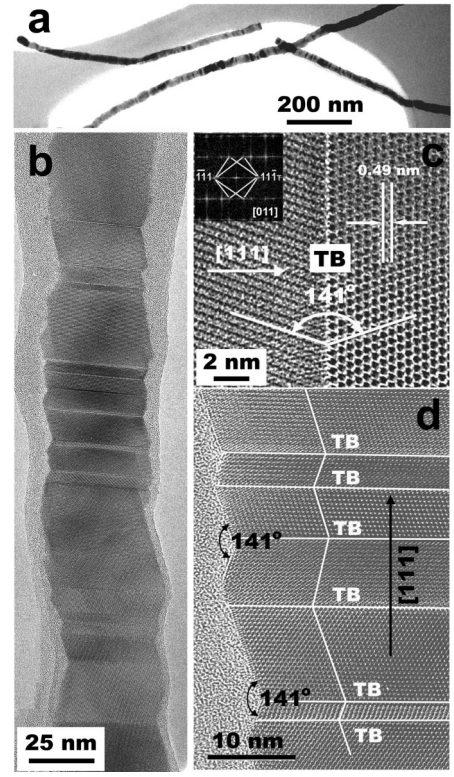

Figure 2. (a, b) TEM images at different magnifications showing the zigzag morphology of Zn_2TiO_4 multitwinned nanowires by solid-state reaction of ZnO/TiO_2 core/shell nanowires at 900 °C for 8 h. Note that the twinning is nonperiodic. (c) A closer view at one twin boundary and the corresponding FFT pattern. (d) Several twinning boundaries with a fixed zigzag angle of 141°.

duced to the range of 30 to 80 nm, which means a reduction by more than 50%. Close observation reveals that the nanowires are composed of large parallelogram-shaped subcrystallites, but do not present periodic stacking (Figure 2b). The high-resolution TEM (HRTEM) images presented in Figures 2c,d reveal that these nanowires consist of phase-pure Zn_2TiO_4 spinel with a face-centered cubic (fcc) crystal lattice structure. Moreover, the zigzag feature originates from multiple microfaceted twin subunits of alternating orientation. The interplanar spacing of 0.49 nm measured in Figure 2c perfectly matches the d_{111} lattice distance of a Zn_2TiO_4 crystal, demonstrating the [111]-oriented growth direction of each individual segment grain. The fast Fourier transform (FFT) pattern of the TB (inset of Figure 2c) indicates clearly a typical (111) twin structure: two mirror planes sharing a common (111) face. No misfit dislocations were observed at the TB interfaces. The linked subunits with diverse thickness are constantly separated by twin planes, resulting in the 1-D multitwinned nanostructure. It is known that (111) twinned crystals have a relative rotational angle of 70.5°. The angle across the TB (Figure 2c) as well as that induced by the sidewall surfaces between the neighboring subunits (Figure 2d) was measured to be ~141°, consistent with both theoretical and experimental values obtained from twinned nanostructures of spinel Zn_2SnO_4 and Zn_2TiO_4,[4,8] as well as cubic binary compounds.

Effect of the Reaction Temperature. As seen in Figure 1b, the deposited TiO_2 film is rather thin compared to the diameters of the ZnO nanowire core. Therefore, the ZnO is present in excess for the reaction between TiO_2 and ZnO, where a Ti/Zn atomic ratio of 1:2 is usually needed to form stoichiometric Zn_2TiO_4.[8,22] However, we still produced phase-pure Zn_2TiO_4 nanowires from the unstoichiometric ZnO/TiO_2 core−shell nanowires under the current annealing conditions. Combined with the fact that the diameters of the starting core−shell nanowires were obviously reduced after the annealing at 900 °C, we considered that a partial "loss" of ZnO should accompany the formation of the multitwinned Zn_2TiO_4 nanowires. To get more details of the involved process, we first lowered the annealing/reaction temperature to 700 °C. A representative morphology of the 1-D nanostructure after annealing at 700 °C for 4 h is shown in Figure 3a. It seems that the surface of the nanowire is inlaid with many individual nanocrystallites, which we name "bricks" according to their appearance. The corresponding electron diffraction (ED) pattern in Figure 3b includes a set of spots from single-crystal hexagonal ZnO with a [0001] growth direction along with polycrystalline diffraction rings from Zn_2TiO_4 spinel. Therefore, the 1-D nanostructure formed at this low temperature condition is a ZnO/Zn_2TiO_4 nanocomposite in which the unconsumed ZnO nanowire core remains while the inlaid bricks on the surface are individual Zn_2TiO_4 nanocrystallites. As mentioned above, amorphous TiO_2 readily crystallizes at a temperature of 300 °C or higher. The initially continuous 5-nm TiO_2 shell on the surface of the ZnO nanowires is expected to transform into anatase TiO_2 islands at the elevating temperature before the commencement of the solid−solid reaction. These islands are loosely interconnected or isolated as a result of volume shrinkage of the amorphous TiO_2 thin film. During the annealing at higher temperatures like 700 °C, the TiO_2 islands could be incorporated in the ZnO lattice as a solid solute at the early stages because of the faster diffusion rate of Ti^{4+} than that of Zn^{2+}.[22] Subsequently, the Zn_2TiO_4 spinel nanocrystallites formed through lattice rearrangement. Unlike the reaction of ZnO−Al_2O_3 nanowires,[23] no voids or tubular structures appeared at the ZnO/Zn_2TiO_4 interface, indicating that the in-diffusion of Ti^{4+} is dominating for the TiO_2/ZnO thermal couple as expected. Consequently, the produced spinel bricks are closely attached to the surface of the unconsumed ZnO nanowire substrates, as shown in Figure 3a.

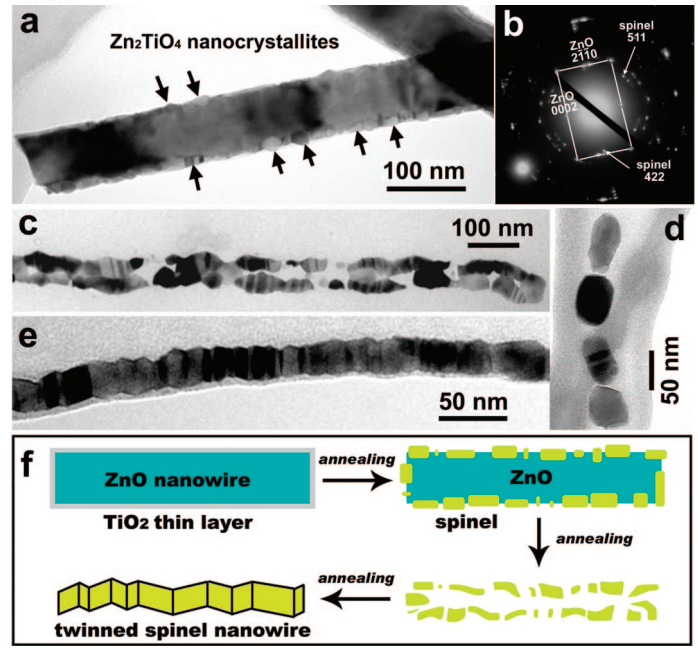

Figure 3. (a, b) TEM image and its corresponding ED pattern of ZnO/TiO_2 core/shell nanowires after annealing at 700 °C for 4 h. Typical TEM images of spinel nanostructures obtained by annealing ZnO/TiO_2 core/shell nanowires at (c, d) 800, and (e) 900 °C for 4 h. (f) Schematic diagram of the growth process for multitwinned Zn_2TiO_4 nanowires from ZnO/TiO_2 core/shell nanowires by annealing at high temperatures.

However, if we adjusted the reaction temperature to 800 °C (with the same duration of 4 h), some multitwinned spinel nanowires were found mixed with the ZnO/Zn_2TiO_4 nanocomposite structure. In addition, a type of fractured 1-D nanostructures (see Figure 3c) was often encountered during TEM observations. These 1-D nanostructures usually contain irregular inner cavities, indicating the loss of the unconsumed ZnO core at higher temperatures.[23] The walls of these structures consist of both multitwinned fragments and untwinned

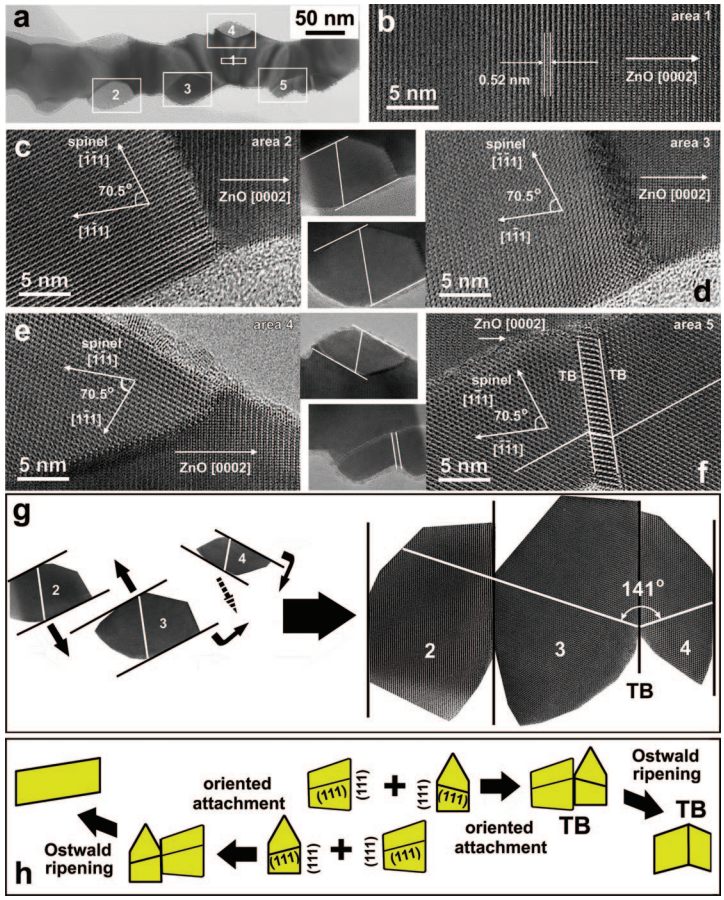

Figure 4. (a) TEM image of an incompletely evolved nanowire after annealing ZnO/TiO_2 core−shell nanowires at 900 °C for 4 h. Magnified views of the areas (b) 1, (c) 2, (d) 3, (e) 4, and (f) 5 marked by the enumerated white frames shown in panel a. (g) Artificial extraction of bricks 2, 3, and 4 from panel a for mimicking the process of the oriented attachment. (h) Schematic diagram of the two assembly modes of different bricks with a pair of exposed (111) surfaces on a (011) basal plane.

ones, which are inclined to assembly into longer aggregates. In some cases one can even identify that some of these individual bricks begin to attach to each other (see Figure 3d). When the annealing was conducted at 900 °C for 4 h, the hollow 1-D nanostructures mostly disappeared, whereas the major result is solid, multitwinned spinel nanowires, as exemplified by the image in Figure 3e.

Formation Mechanism. On the basis of the above investigations, we propose the following. The formation of the multitwinned Zn_2TiO_4 nanowires by annealing the ZnO/TiO_2 core−shell nanowires at 900 °C involves overall multiple stages: First, spinel Zn_2TiO_4 nanobricks form on the surface of the ZnO nanowires. Subsequently, the unconsumed ZnO core is desorbed or evaporated through the gaps of the bricks, very much like a chemical desorption of surface atoms of Zn−O.[23−25] Lastly, the remaining loosely connected bricks tend to attach to each other, coalesce, and finally evolve into the multitwinned spinel nanowires. This formation process is schematically illustrated in Figure 3f.

The oriented attachment of preformed crystals had already been suggested as an important mechanism for the formation of twins.[26] Penn *et al.* revealed that an imperfectly oriented attachment in solution can give rise to crystals separated by twin boundaries or other planar defects. This also well explains the twins frequently observed in natural and synthetic nanocrystallites.[27,28] However, the oriented attachment of nanocrystallites more possibly led to the formation of single crystalline nanowires/nanorods or those with dislocations and infrequent TBs in some cases.[29] Therefore, the appearance of the multitwinned nanowires observed here requires further elucidation.

Figure 4a shows an incompletely evolved nanowire after annealing the ZnO/TiO_2 core−shell nanowires at 900 °C for 4 h. The stem and several inlaid bricks are marked as 1, 2, 3, 4, and 5, respectively. The residual stem consists of the single-crystal ZnO nanowire which maintains its original orientation (Figure 4b) though its surface has been dramatically modified. Figure 4 panels c, d, e, and f present HRTEM images of the respective bricks 2, 3, 4, and 5, in conjunction with each corresponding overview. Although every Zn_2TiO_4 spinel brick tightly contacts the ZnO stem, there exist grain boundaries at the ZnO/Zn_2TiO_4 interfaces. Therefore, an epitaxial growth relationship cannot be established. However, all these spinel bricks are aligned on a (011) basal plane. Bricks 2, 3, and 4 are facetted and at least show a couple of exposed (111) parallel surfaces.[6,30] This is reasonable since the (111) facet has the lowest surface energy for an fcc structure. Accordingly, the (111) plane is usually the dominant facet enclosing the crystal. Interestingly, twin boundaries have already been formed in some bricks like brick 5 for instance shown in Figure 4f. We assume that the TB formation as in brick 5 most probably happened during the spinel nucleation stage. Compared with ordinary plane nucleation, the TB formation is energetically less favored. However, this energy barrier might be easily overcome owing to the relatively low twin-plane energy. Consequently, twin-plane nucleation could be induced by different factors involved in accidental departure from minimal energy conditions such as impurity incorporation, mass fluctuations, and thermal fluctuations during annealing.[6]

It is reasonable to assume that, with further desorption or evaporation of the unconsumed ZnO stem, the quasi-1-D ZnO/Zn_2TiO_4 composite structure will gradually collapse. As a result, the individual spinel bricks with compatible surfaces will approach each other. When two bricks come into contact with a random orientation, they tend to rearrange their orientation and achieve an oriented attachment. The driving force is a reduction of free surface energy by forming chemical bonds between opposite surface atoms for complete removal of pairs of surfaces.[31] For mimicking this process, we artificially extracted bricks 2, 3, and 4 from Figure 4a and show the individual crystallites. As illus-

trated in Figure 4g,h, the oriented attachment along the [111] axis among these bricks has two possibilities. If only a planar rotation is considered, the (111)-oriented attachment between bricks 2 and 3 will produce a larger single-crystal spinel brick. In contrast, the attachment between bricks 3 and 4 leads to the formation of a twin boundary. The probability of both events is equal, so the nonperiodic multitwinned Zn_2TiO_4 nanowires are finally shaped through the linear brick aggregations stochastically following these two modes, as simulated in Figure 4g.

Sunagawa and Tomura in 1976 suggested the term "flying magic carpets", to indicate the moving of thin lamellar phlogopite crystals in the crystallization medium (lavas) while they are growing, which leads to multi-individual twins of widely different sizes.[32] The mechanism of twin formation in our system is partly similar to this one. However, our bricks cannot "fly" freely. Their "flying" directions are basically determined by the 1-D ZnO template. It should be noted that in addition to short-range interactions between the adjacent surfaces, rotations of approaching nanoparticles in solution might also be driven by Brownian motion, which is favorable for the "bricks" to find the lowest-energy configuration between the adjacent surfaces,[33] so the chance for formation of multitwinned nanowires in solutions is low. In contrast, during the solid−solid reaction in our experiment, the adequate rotation of the bricks within aggregates will be severely restricted. Therefore, the multiple TB can survive as the second lowest energy configuration. Because of the rapid agglomeration of the spinel bricks at the high temperature, the attachment among the bricks cannot exclusively happen in a well-oriented manner. As shown in Figure 5, we can also detect other defects such as grain boundaries mixed with the TB in some Zn_2TiO_4 nanowires.

Comparing the model we suggest (Figure 4 panels g and h) with the actual multitwinned Zn_2TiO_4 nanowires (Figure 2), it can be seen that the bottlenecks between the adjacent spinel bricks must have been filled up. Moreover, the exposed surfaces of each subunit were also smoothed and reconstructed in the final structure. This process most likely occurs during the final stage, which involves an Ostwald ripening process following conventional mechanisms of dissolution and growth of monomers, as illustrated in Figure 4h.[29]

Formation of Nanobricks by e-Beam Irradiation. Another interesting phenomenon is the formation of spinel nanobricks induced by the electron beam irradiation. During the TEM observation of the multitwinned Zn_2TiO_4 nanowires, we noticed the gradual appearance of many tiny nanocrystallites on the exposed surfaces of the nanowires. The HRTEM image shown in Figure 6a presents several nuclei of nanocrystallites attached to the exposed (111) surfaces of each subunit. Careful TEM analysis of their structure (Figure 6b) confirms that all these new nanocrystallites are cubic spinel-phase Zn_2TiO_4. To further investigate the evolution of these nanocrystallites, we irradiated the Zn_2TiO_4 nanowires by electron beam operating at 400 kV in TEM for a designated duration. TEM images in Figure 6c,d show the surface structure of a multitwinned nanowire after beam irradiations over a time of 12 and 28 min, respectively. High-magnification views of the nanowire surface in the identical area (marked by the black frame in Figure 6 panels c and d) are shown in Figure 6 panels e and f, respectively. Two main changes can be easily identified (indicated by the arrows): First, the nanowire was decorated with numerous tiny nano-

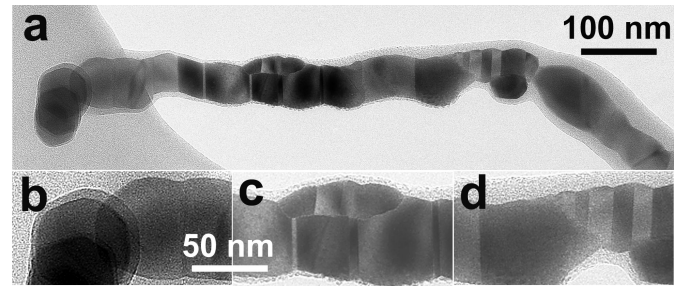

Figure 5. (a−d) TEM images of other defects like grain boundaries mixed with TB in some 1-D Zn_2TiO_4 nanowires.

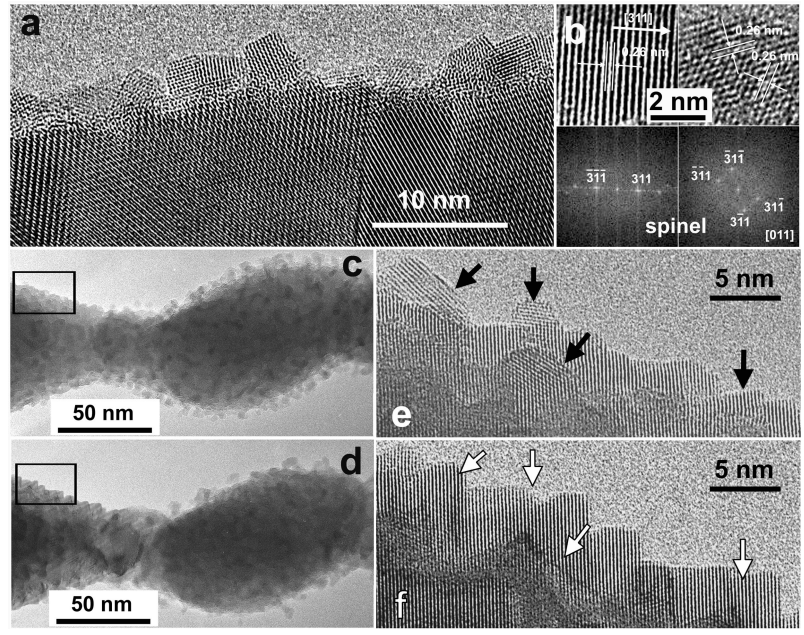

Figure 6. (a) TEM image of a multitwinned Zn_2TiO_4 nanowire attached with many nucleated nanocrystallites while exposed to the electron beam for some time. (b) TEM images and their corresponding FFT patterns showing that these tiny nanocrystallites are Zn_2TiO_4 spinel. TEM images of a multitwinned Zn_2TiO_4 nanowire after approximately (c) 12 and (d) 28 min exposure in the electron beam produced at 400 kV accelerating voltage. (e, f) Magnified views of the area respectively selected from panels c and d marked by the black frame. The arrows illustrate the change in the size of the nanocrystallites and surface flatness of the nanowire.

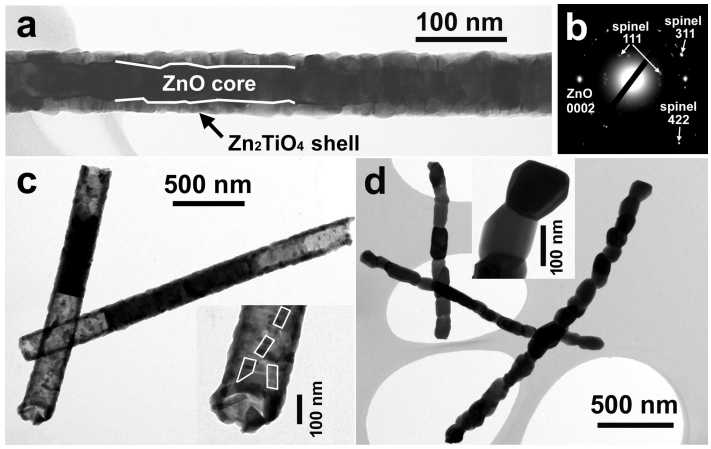

Figure 7. (a, b) TEM image and its corresponding ED pattern of ZnO nanowires shelled by a ~17 nm TiO_2 film after annealing at 700 °C for 4 h. (c) Tubular Zn_2TiO_4 structures after a partial removal of the unconsumed ZnO core. Note that only local TB structures are observed as marked by white boxes. (d) TEM image of ZnO nanowires shelled by a ~17 nm TiO_2 film after annealing at 800 °C for 4 h. Grain boundaries between adjacent bricks are clearly presented.

particles after 12-min irradiation. The number of the attached nanocrystallites significantly dropped after the irradiation time was extended to 28 min. Second, while some nanocrystallites started to epitaxially fuse into the nanowire, edge and screw dislocations were synchronously produced (Figure 6e). After 28-min electron beam irradiation, the number of such dislocations was reduced and the nanowire surface became crystallographicly flatter (Figure 6f). The above results demonstrate that a larger single-crystalline subunit can be gradually formed by fusing the attached nanocrystallites into the stem over elongated e-beam irradiation.

We consider that the high energy of the electron beam in TEM induces the decomposition of metastable or small spinel nanocrystallites in the annealed products because of their higher chemical potential. The monomers are thus produced and then attached to the exposed surfaces of the nanowires, which leads to the new nucleation of many spinel nanocrystallites. The multitwinned Zn_2TiO_4 nanowires can thus grow at the expense of the attached spinel nanocrystallites. Though this irradiation mechanism might be somewhat different from the thermal approach on crystal growth *via* Ostwald ripening, we believe a similar process happens during the final assembly stage of the spinel individuals at high temperatures, that is, the multitwinned Zn_2TiO_4 nanowires with all the exposed (111) surfaces are finally developed *via* Ostwald ripening after the oriented attachment of "imperfect" bricks.

Larger TiO_2 Layer Thickness. Formation of the multitwins depends also on the thickness of the TiO_2 layer. In above experiments, all the TiO_2 thicknesses were 5 nm, which is a skinny layer relative to the diameter of the ZnO nanowire core (60−200 nm). In a control experiment, we deposited a TiO_2 layer of ~17 nm on the ZnO nanowire template by increasing the number of ALD cycles and annealed this ZnO/TiO_2 core−shell nanowire sample at various temperatures. Figure 7a shows a typical TEM image of the sample after annealing at 700 °C for 4 h. A core−shell nanowire with a rugged interface is now observed. The corresponding ED pattern (Figure 7b) and the other morphology characterizations (not shown here) confirm that this 1-D structure is a ZnO nanowire core surrounded by a continuous Zn_2TiO_4 nanoparticulate film. Obviously, the amount of 17-nm TiO_2 layer is still insufficient for the complete consumption of ZnO core during the solid−solid reaction. However, in contrast to the product resulting from the 5-nm TiO_2 layer, the size of the Zn_2TiO_4 crystallites in the shell is much larger and no intervals exist between them. To further investigate the structure of the Zn_2TiO_4 shell, we released the Zn_2TiO_4 shells by dissolving the unconsumed ZnO core in a dilute hydrochloric acid solution (0.01 M). Figure 7c shows such a hollow structure after partial dissolution of the ZnO core. The tubular section generally presents a polycrystalline structure. Though we can also detect some areas including the TB, as marked by the white frames, no long-range lamellar twinning is found.

When the core−shell nanowires with a ~17 nm TiO_2 layer were annealed at 800 or 900 °C for 4 h, no multitwinned spinel nanowires were observed; instead the nanowires are composed of grains. Figure 7d shows a representative TEM image of the sample after annealing at 800 °C for 4 h. Like before, all the unconsumed ZnO was desorbed at this high temperature and only the phase-pure spinel nanowires remained. However, the formed 1-D nanowires consist of big spinel bricks joined by grain stacking rather than TB.

An active oriented attachment usually depends on an environment favoring the motion and casual interaction of the preformed crystals, that is, the crystals should somehow be free for moving and interacting.[26,31] When the thickness of the TiO_2 layer was increased from 5 to 17 nm, the solid−solid reaction with the thicker TiO_2 shell not only produced larger spinel bricks, but also partly eliminated the space between the bricks. Therefore, the individual bricks will be maintained in their original orientation because of steric hindrance to reorientation. The "frozen" orientations mostly prevented the oriented attachment of the adjacent or approaching spinel bricks during the subsequent assembly process. This is in qualitative consistency with the conclusion by Penn *et al.*,[34] that the overall rate constant for growth by oriented aggregation decreases noticeably with increasing primary crystal size. Therefore, most of these larger bricks aggregated into the 1-D nanostructure without showing the same crystallographic orientation and thus no multitwinned Zn_2TiO_4 nanowires were formed. It is expected that, with further increases in the TiO_2 layer thickness, the whole reaction process will be more like the conventional solid-state reaction of powder oxide mixtures,

where grain boundaries dominate twin boundaries in the final structure.

CONCLUSIONS

Multitwinned Zn_2TiO_4 nanowires have been synthesized *via* a solid-state reaction of ZnO nanowires with a 5-nm TiO_2 shell. On the basis of experimental results from different reaction temperatures and durations, and careful TEM investigations, we propose that the multitwinned nanostructures develop *via* an oriented attachment of preformed spinel nanobricks. Specifically, three steps are involved during the annealing: first, the initially continuous 5-nm amorphous TiO_2 shell on the surface of ZnO nanowires transforms into anatase TiO_2 islands, which are isolated from each other as a result of crystallization-induced volume shrinkage. Second, the TiO_2 is incorporated into the ZnO lattice as segregation and reacts into individual spinel crystallites through lattice rearrangement. These spinel bricks are attached to the surface of the unconsumed ZnO stem. Finally, the unreacted ZnO is decomposed and evaporated through the gaps of the bricks, leaving a chain of loose-interconnected bricks. The bricks will then assemble into solid multitwinned nanowires *via* an oriented attachment and coalescence (Ostwald ripening).

Overall, the ZnO nanowires function not only as a reactant, but also as a navigational template for the liner assembly of the individual bricks. More importantly, the intervals among the starting bricks as well as the space created by desorption of the unconsumed ZnO core was verified essential to the motion and reorientation of the preformed bricks to achieve an efficient oriented attachment. In this study we provided direct experimental evidence for these important points through careful TEM observations.

EXPERIMENTAL SECTION

ZnO nanowires were grown by vapor-phase transport in a double-tube furnace using a source material consisting of a mixture of ZnO and graphite powder in a weight ratio of 1:1.[19] In brief, the source material was loaded into an alumina boat at the high-temperature zone (925 °C), while a cleaned silicon substrate with Au nanoparticle catalysts was placed downstream of the Ar flow at the low-temperature zone (750 °C) for harvesting the ZnO nanowires. Typically the maximum temperature was kept under a constant Ar flow of 30 standard cubic centimeters per minute (sccm) for 30 min. The furnace was naturally cooled down to room temperature after the growth.

The as-prepared ZnO nanowires were then transferred into an ALD chamber. ZnO/TiO_2 core−shell nanowires were fabricated by ALD deposition of a TiO_2 film on the ZnO nanowires using titanium tetraisopropyl oxide ($Ti[OCH(CH_3)_2]_4$, TIP) and water as Ti precursor and oxygen reactant sources, respectively. Ar flow served as both the carrier of the precursors and the purging gas. The deposition was conducted with a substrate temperature of 100 °C and a background pressure of 0.15 Torr. We used a total number of 300 cycles to obtain TiO_2 films with a thickness of ~5 nm. We also deposited TiO_2 films with a thickness of ~17 nm by increasing the ALD cycles to 1500 for a control experiment.

The ZnO/TiO_2 core−shell nanowires were then annealed in an open quartz tube furnace at 900 °C for 8 h to induce the interfacial solid state reaction for the formation of zinc titanate. Annealing was also carried out at 700 and 800 °C or a shorter time to trace the process of this solid−solid reaction.

The obtained nanostructures were characterized and analyzed using TEM (JEOL, JEM-1010; Philips, CM20T), and high-resolution TEM (JEOL, JEM-4010). *In-situ* morphology evolution of the Zn_2TiO_4 nanowires at different electron beam irradiation duration was performed in the JEM-4010 TEM microscope.

Acknowledgment. This work was supported by Deutsche Forschungsgemeinschaft (DFG) under contract numbers Za 191/23-1and HE 2100/8-1 and the German Federal Ministry of Education and Research (BMBF) in the frame of DIP.

REFERENCES AND NOTES

1. Cahn, R. W. Twinned Crystals. *Adv. Phys.* **1954**, *3*, 202–445.
2. Shen, P.; Lee, W. H. (111)-Specific Coalescence Twinning and Martensitic Transformation of Tetragonal ZrO_2 Condensates. *Nano Lett.* **2001**, *1*, 707–711.
3. Li, Q.; Gong, X. G.; Wang, C. R.; Wang, J.; Ip, K. M.; Hark, S. K. Size-Dependent Periodically Twinned ZnSe Nanowires. *Adv. Mater.* **2004**, *16*, 1436–1440.
4. Chen, H.; Wang, J.; Yu, H.; Yang, H.; Xie, S.; Li, J. Transmission Electron Microscopy Study of Pseudoperiodically Twinned Zn_2SnO_4 Nanowires. *J. Phys. Chem. B* **2005**, *109*, 2573–2577.
5. Korgel, B. A. Twins Cause Kinks. *Nat. Mater.* **2006**, *5*, 521–522.
6. Johansson, J.; Karlsson, L. S.; Svensson, C. P. T.; Mårtensson1, T.; Wacaser, B. A.; Deppert, K.; Samuelson, L.; Seifert, W. Structural Properties of κB-Oriented III−V Nanowires. *Nat. Mater.* **2006**, *5*, 574–580.
7. Davidson, F. M.; Lee, D. C.; Fanfair, D. D.; Korgel, B. A. Lamellar Twinning in Semiconductor Nanowires. *J. Phys. Chem. C* **2007**, *111*, 2929–2935.
8. Yang, Y.; Sun, X. W.; Tay, B. K.; Wang, J. X.; Dong, Z. L.; Fan, H. M. Twinned Zn_2TiO_4 Spinel Nanowires Using ZnO Nanowires as a Template. *Adv. Mater.* **2007**, *19*, 1839–1844.
9. Zhang, Z. H.; Wang, F. F.; Duan, X. F. Formation Mechanism of Pseudoperiodical Multi-Twinning Nanostructures. *J. Cryst. Growth* **2007**, *303*, 612–615.
10. Tao, X. Y.; Li, X. D. Catalyst-Free Synthesis, Structural, and Mechanical Characterization of Twinned $Mg_2B_2O_5$ Nanowires. *Nano Lett.* **2008**, *8*, 505–510.
11. Chen, K.-C.; Wu, W.-W.; Liao, C.-N.; Chen, L.-J.; Tu, K. N. Observation of Atomic Diffusion at Twin-Modified Grain Boundaries in Copper. *Science* **2008**, *321*, 1066–1069.
12. Cui, Y.; Wei, Q. Q.; Park, H. K.; Lieber, C. M. Nanowire Nanosensors for Highly Sensitive and Selective Detection of Biological and Chemical Species. *Science* **2001**, *293*, 1289–1292.
13. Xia, Y. N.; Yang, P. D.; Sun, Y. G.; Wu, Y. Y.; Mayers, B.; Gates, B.; Yin, Y. D.; Kim, F.; Yan, Y. One-Dimensional Nanostructures: Synthesis, Characterization, and Applications. *Adv. Mater.* **2003**, *15*, 353–389.
14. Fan, H. J.; Werner, P.; Zacharias, M. Semiconductor Nanowires: From Self-Organization to Patterned Growth. *Small* **2006**, *2*, 700–717.
15. Yi, G.; Schwarzacher, W. Single Crystal Superconductor Nanowires by Electrodeposition. *Appl. Phys. Lett.* **1999**, *74*, 1746–1748.
16. Bietsch, A.; Michel, B. Size and Grain-Boundary Effects of a Gold Nanowire Measured by Conducting Atomic Force Microscopy. *Appl. Phys. Lett.* **2002**, *80*, 3346–3348.

17. Youngdahl, C. J.; Weertman, J. R.; Hugo, R. C.; Kung, H. H. Deformation Behavior in Nanocrystalline Copper. *Scr. Mater.* **2001**, *44*, 1475–1478.
18. Knez, M.; Niesch, K.; Niinistö, L. Synthesis and Surface Engineering of Complex Nanostructures by Atomic Layer Deposition. *Adv. Mater.* **2007**, *19*, 3425–3438.
19. Fan, H. J.; Fuhrmann, B.; Scholz, R.; Himcinschi, C.; Berger, A.; Leipner, H.; Dadgar, A.; Krost, A.; Christiansen, S.; Gösele, U.; Zacharias, M. Vapour-Transport-Deposition Growth of ZnO Nanostructures: Switch between *c*-Axial Wires and *a*-Axial Belts by Indium Doping. *Nanotechnology* **2006**, *17*, S231–S239.
20. Tan, L. K.; Chong, M. A. S.; Gao, H. Free-Standing Porous Anodic Alumina Templates for Atomic Layer Deposition of Highly Ordered TiO_2 Nanotube Arrays on Various Substrates. *J. Phys. Chem. C* **2008**, *112*, 69–73.
21. King, D. M.; Liang, X. H.; Carney, C. S.; Hakim, L. F.; Li, P.; Weimer, A. W. Atomic Layer Deposition of UV-Absorbing ZnO films on SiO_2 and TiO_2 Nanoparticles Using a Fluidized Bed Reactor. *Adv. Funct. Mater.* **2008**, *18*, 607–615.
22. Manik, S. K.; Bose, P.; Pradhan, S. K. Microstructure Characterization and Phase Transformation Kinetics of Ball-Milled Prepared Nanocrystalline Zn_2TiO_4 by Rietveld Method. *Mater. Chem. Phys.* **2003**, *82*, 837–847.
23. Yang, Y.; Kim, D. S.; Knez, M.; Scholz, R.; Berger, A.; Pippel, E.; Hesse, D.; Gösele, U.; Zacharias, M. Influence of Temperature on Evolution of Coaxial ZnO/Al_2O_3 One-Dimensional Heterostructures: From Core−Shell Nanowires to Spinel Nanotubes and Porous Nanowires. *J. Phys. Chem. C* **2008**, *112*, 4068–4074.
24. Fan, H. J.; Lotnyk, A.; Scholz, R.; Yang, Y.; Kim, D. S.; Pippel, E.; Senz, S.; Hesse, D.; Zacharias, M. Surface Reaction of ZnO Nanowires with Electron-Beam Generated Alumina Vapor. *J. Phys. Chem. C* **2008**, *112*, 6770–6774.
25. Yang, Y.; Scholz, R.; Berger, A.; Kim, D. S.; Knez, M.; Hesse, D.; Gösele, U.; Zacharias, M. Transmission Electron Microscopy *in-Situ* Fabrication of ZnO/Al_2O_3 Composite Nanotubes by Electron-Beam Irradiation Induced Local Etching of ZnO/Al_2O_3 Core-Shell Nanowires. *Small* **2008**, *4*, 2112–2117.
26. Nespolo, M.; Ferraris, G. The Oriented Attachment Mechanism in the Formation of Twins—A Survey. *Eur. J. Mineral.* **2004**, *16*, 401–406.
27. Penn, R. L.; Banfield, J. F. Imperfect Oriented Attachment: Dislocation Generation in Defect-Free Nanocrystals. *Science* **1998**, *281*, 969–971.
28. Penn, R. L.; Banfield, J. F. Oriented Attachment and Growth, Twinning, Polytypism, and Formation of Metastable Phases: Insights from Nanocrystalline TiO_2. *Am. Mineral.* **1998**, *83*, 1077–1082.
29. Pacholski, C.; Kornowski, A.; Weller, H. Self-Assembly of ZnO: From Nanodots to Nanorods. *Angew. Chem., Int. Ed.* **2002**, *41*, 1188–1191.
30. If we consider that the bricks actually have a complex 3-D structure like "truncated" octahedral, more (111) planes are possibly exposed on the brick surfaces.
31. Penn, R. L. Kinetics of Oriented Aggregation. *J. Phys. Chem. B* **2004**, *108*, 12707–12712.
32. Sunagawa, I.; Tomura, S. Twinning in Phlogopite. *Am. Mineral.* **1976**, *61*, 939–943.
33. Banfield, J. F.; Welch, S. A.; Zhang, H.; Ebert, T. T.; Penn, R. L. Aggregation-Based Crystal Growth and Microstructure Development in Natural Iron Oxyhydroxide Biomineralization Products. *Science* **2000**, *289*, 751–754.
34. Penn, R. L.; Tanaka, K.; Erbs, J. Size Dependent Kinetics of Oriented Aggregation. *J. Cryst. Growth* **2007**, *309*, 97–102.